

# Preparation and Properties of Compatibilized PVC/SMA-g-PA6 Blends

Lijie Dong, Chuanxi Xiong, Tao Wang, Dan Liu, Shengjun Lu, Yinzhen Wang

School of Materials Science and Engineering, Wuhan University of Technology, Wuhan 430070, People's Republic of China

Received 30 October 2003; accepted 3 April 2004

DOI 10.1002/app.20724

Published online in Wiley InterScience (www.interscience.wiley.com).

**ABSTRACT:** The morphology and mechanical properties of PVC/SMA-g-PA6 blends were investigated in this paper. Graft to polymer SMA-g-PA6 was prepared via a solution graft reaction between SMA and PA6. FTIR test evidences the occurrence of the graft reaction between SMA and PA6. DSC analysis shows that SMA-g-PA6 has a lower melting point of 187°C, which may result in a decrease in crystallinity of PA6 and thus enable efficient blending of SMA-g-PA6 and PVC. Compatibilization was evidenced by the dramatic

increase in mechanical properties, the smaller particle size and finer dispersion of PA6 in PVC matrix, and, further, a cocontinuous morphology at 16 wt % SMA-g-PA6 content. SMA-g-PA6 from the solution graft reaction can toughen and reinforce PVC material. © 2004 Wiley Periodicals, Inc. *J Appl Polym Sci* 94: 432–439, 2004

**Key word:** nylon 6; poly(vinyl chloride) (PVC); graft copolymers; compatibilization

## INTRODUCTION

Poly(vinyl chloride) (PVC) is a widely used thermoplastic due to its exceptional corrosion resistance, self-extinguishability, flame resistance, inexpensiveness, and recoverability. But PVC has moderate impact resistance, bad processing properties, and thermal resistance. The enhancement of its performance to engineering materials standard has received considerable attention for many years. Numerous studies have been devoted to toughen and reinforce PVC by the addition of inorganic filler or organic elastomer.

Polyamide 6 (PA6) has been one of the most widely used engineering thermoplastics since the I.G. Farbenindustrie commercially developed it about 1940. It has several distinctive engineering properties, such as elasticity, mechanical properties, stiffness, abrasion resistance, oil resistance, and chemical resistance. As a polar polymer, PA6 absorbs water easily and, consequently, impact strength, elastic modulus, and dimensional stability deteriorate. Means of modification include blending, filling, copolymerization, and use in a nanocomposite.

Polymer blending has already been established as an effective means for constructively altering trans-

port properties of polymeric material. The end-use properties of these polymer blends are mainly dependent on the compatibility that develops during processing. Before modification, PVC/PA6 blends have obviously poorer impact and tensile strength because of the incompatibility of nonpolar PVC and polar PA6. The diversity of the solvent interaction parameter between PA6 ( $\delta = 13.6$ ) and PVC ( $\delta = 9.7$ ) is another reason for their poor compatibility and bad interfacial adhesion, which would certainly lead to easy fracture of the blends. The processing temperature of PVC is  $\sim 170$ – $190^\circ\text{C}$ , whereas the melting point of nylon 6 is  $215^\circ\text{C}$ . The huge difference of their processing temperatures becomes the main obstacle to the blending of PVC and PA6. There are few papers related to the blending of PVC and PA6.

In the middle of the 20<sup>th</sup> century, Dupont Packaging & Industrial Polymers produced PVC/PA6 blends, by using EnBACO(ethylene-acrylate-*co* copolymer) and EnBACO-MAH(maleic anhydride grafted EnBACO) as compatibilizers, and commercially developed several PVC/nylon blends: PA6/PVC, PA12/PVC, PA1212/PVC, etc.<sup>1–5</sup> Cybertech Co. in the United States used EnBACO-developed PA/PVC alloy with the trade name of Cylon.<sup>6</sup>

Lian et al.<sup>7</sup> compatibilized amorphous nylon terpolymer and PVC by EnBACO (ethylene-acrylate-*co* copolymer) and EnBACO-MAH (maleic anhydride grafted EnBACO), thus a new PVC/PA alloy was born. SEM reveals that the PVC/NT blends have a two-phase structure and the NT phase is the continuous phase while the PVC/NT ratio varies from 72/25 to 25/75. EnBACO and EnBACO-g-MAH have some

Correspondence to: C. X. Xiong (polymerlab@mail.whut.edu.cn; xchuanxi@public.wh.hb.cn).

Contract grant sponsor: the National High Technology Research and Development Program of China (863 Program) Contract grant number: 2002AA333110

effects on the glass transition of PVC and cold crystallization of NT in PVC/NT blends. The effects of compatibilizers on the properties and structures and the mechanism of compatibilizing effects were also investigated.<sup>7-9</sup>

This investigation is focused on a study of the performance and the compatibility of PVC and PA6 using SMA (styrene-maleic anhydride copolymer) as a grafting modifier to reduce the tacticity of the PA6 molecular structure and consequently to give relatively lower crystallinity and melting point ( $T_m$ ) of the PA6. The factors affecting the lower  $T_m$  of PA6 during the grafting of SMA onto PA6 are also discussed.

## EXPERIMENTAL

### Raw materials

Poly(vinyl chloride) was provided by Sinopec Qilu Co., Ltd. (China) in the form of powder with a  $M_w$  of  $6.25 \times 10^4$ . Polyamide 6 homopolymer resin was provided by Monsanto Co. with a molecular weight of  $2.7 \times 10^4$ . Styrene-maleic anhydride copolymer was provided by DSM Co. (Harland); other additives are commercial products.

### Grafting reaction treatment

The grafting reaction was performed in a ternary flask. PA6 was added to phenol with continuous stirring until the PA6 was dissolved. SMA was then added to the reactor under nitrogen atmosphere. The reaction was allowed to proceed for several hours at 80°C under stirring. After reaction, the phenol was removed by distillation, and the coarse product then was cooled to 25°C and extracted 24 h in a Soxhlet apparatus with acetone as the extraction solvent, and was finally dried in an oven under vacuum at 50°C for 24 h.

### Sample preparation and testing

PVC, SMA-g-PA6, and other additives were premixed proportionally in a mixing machine and were removed to mix in the internal mixer (XSS-300) at 185°C and 80 rpm for 10 min and then were compressed to thick sheets through an external mixer (XLS-160). After that, 4-mm-thick sheets of these blends were made by compression molding ( $350 \times 350 \times 2$ ) for impact tests.

Izod impact specimens were prepared according to ASTM D4812. Izod impact strength was obtained from unnotched specimens using an impact tester (JB6): an impact velocity of 3.4 m/s was used. Tensile properties were measured according to ASTM D638 using a tensile tester (RDT-30A) with computerized data acquisition. The testing was generally performed at a cross-head speed of 20 mm/min at ambient conditions (20~25°C and 30~40% RH).

## Characterization

First, the synthesized SMA-g-PA6 was extracted 24 h in the Soxhlet apparatus, with acetone as extraction solvent, to remove the unreacted SMA. After this, samples were dried in an oven under vacuum at 50°C for 24 h. The synthesized SMA-g-PA6 and KBr then were thoroughly mixed and pressed into thick films using a compression molding machine between two Teflon sheets at 180°C, at a load of 10 tons, for a 5-min period. Finally, samples were analyzed using an FTIR spectrometer (Nicolet 20DXB model spectrometer, Madison, WI).

Solid-state  $^{13}\text{C}$  NMR were recorded in a Bruker AMX-400 spectrometer at 298 K, to analyze the solid residues after the grafting reaction treatment. The magic angle spinning rate was 7 KHz, the 90° pulse on carbons and protons was 5  $\mu\text{s}$ . The Toss method was used for suppressing spinning side bands.

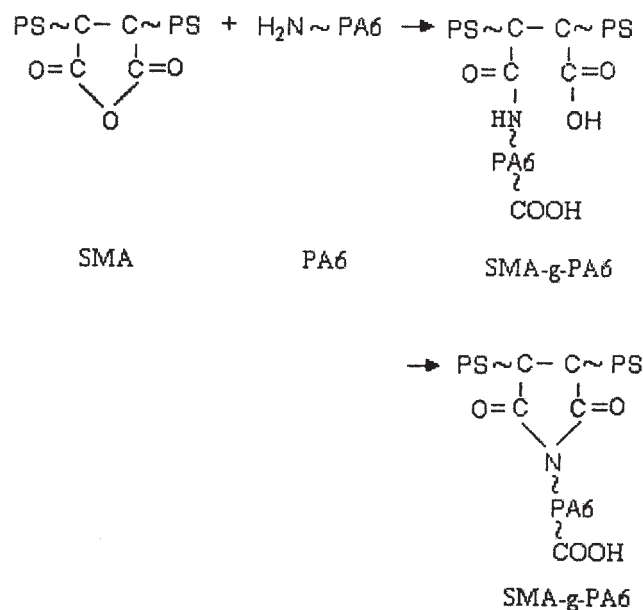
Differential scanning calorimetry testing was completed in a Perkin-Elmer DSC at a heating rate of 20°C/min. The recorded scans during the second heating were analyzed in terms of melting point.

Scanning electron microscopy examination was made under a JSM-5610LU scanning electron microscope (Tokyo, Japan). Prior to SEM examination, the surfaces were coated with a layer of palladium.

## RESULTS AND DISCUSSION

### Grafting reaction

The grafting reaction is shown below:



### Fourier transform infrared spectroscopy

Figure 1 is the spectrum of pure PA6. Figure 2 is the spectrum of SMA-g-PA6 residue, the peaks at 1,778

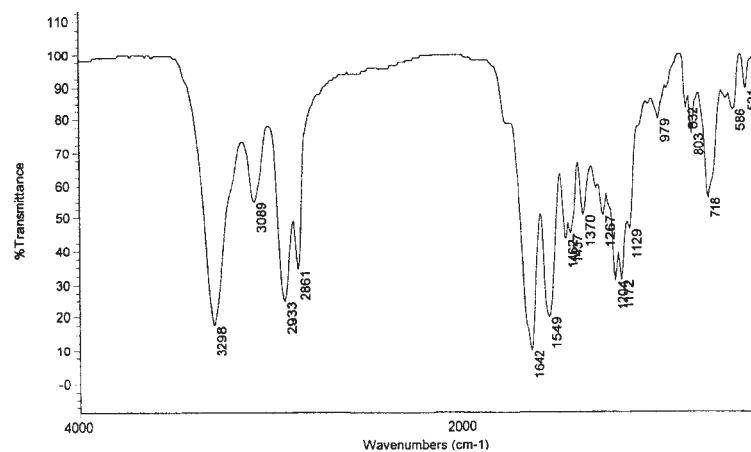


Figure 1 FTIR spectrum of neat PA6.

and  $1,856\text{ cm}^{-1}$ , which belong to the  $\text{—CO—}$  stretching vibration of SMA, appear in the spectrum. This confirms the occurrence of the grafting reaction of SMA to PA6. For comparison, a mixture of PA6 and SMA, without reaction, was also extracted by acetone for 24 h in a Soxhlet apparatus and the resulting powder was analyzed by FTIR spectrometer. The spectrum is shown in Figure 3. It can be seen from the spectrum that there are no peaks at  $1,778$  or  $1,856\text{ cm}^{-1}$ , which indicates the absence of MA groups. The peaks in the spectrum are all PA6 characteristic absorption peaks. This is because the nonreacted SMA in the mixture was extracted out by acetone.

#### Solid-state NMR analysis

Figure 4 shows the CP/MAS  $^{13}\text{C}$  NMR spectrum of SMA. The resonance peak at  $172.6\text{ ppm}$  belongs to

the  $\text{—CO—}$  group of SMA, the broad peak at  $126.1\text{ ppm}$  is the resonance peak of carbon atom in the phenyl, and the broad peak at about  $39.1\text{ ppm}$  is the carbon resonance in the main chain of SMA. Figure 5 is a typical  $^{13}\text{C}$  NMR spectrum of PA6, in which the peak at  $170.7\text{ ppm}$  corresponds to the  $\text{—CO—}$  of PA6. After the grafting of SMA onto PA6, the spectrum of PA6 was markedly changed as shown in Figure 6. First, a new resonance peak appears at about  $124.1\text{ ppm}$ , which corresponds to the carbon in the phenyl of SMA, shifting about  $2\text{ ppm}$  relative to pure SMA. Another new broad peak appears at  $40.6\text{ ppm}$ , which is the carbon resonance in the backbone of SMA. For comparison, the spectrum of the mixed unreacted PA6 and SMA after 24 h extraction by acetone is given in Figure 7: this spectrum shows no resonance peak of SMA, which had been removed by acetone during

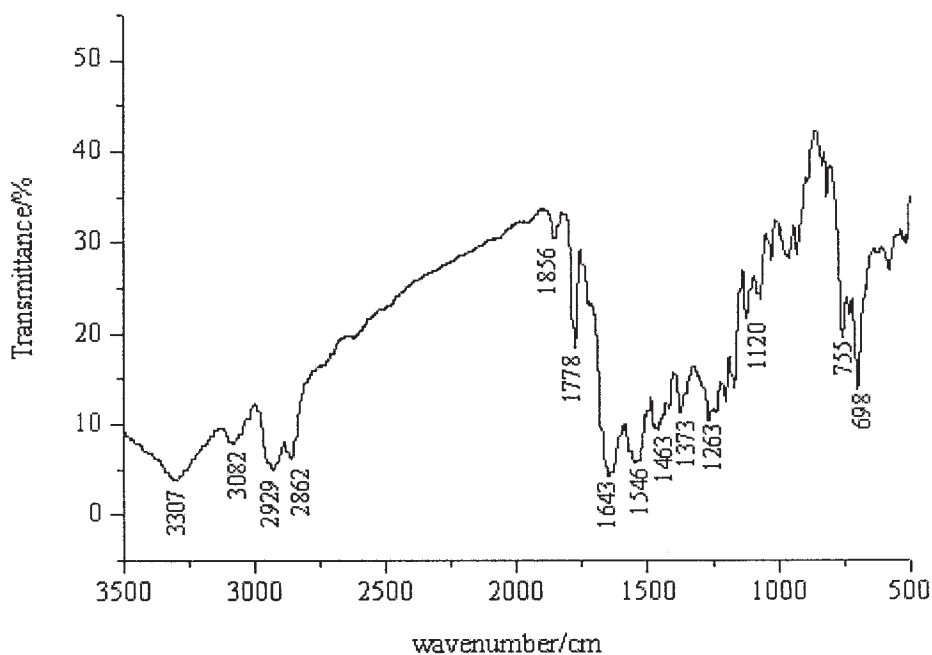


Figure 2 FTIR spectrum of SMA-g-PA6 copolymer.

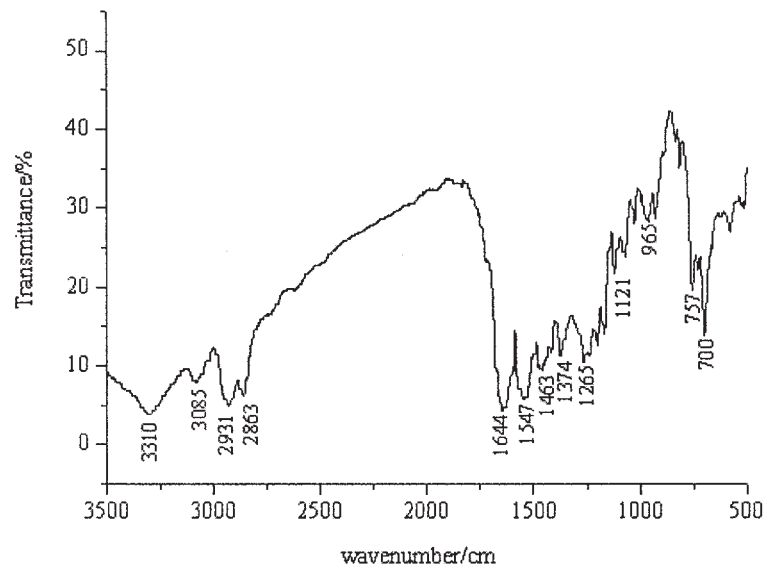


Figure 3 FTIR spectrum of SMA and PA6 mixer after being extracted with a Soxhlet apparatus by acetone.

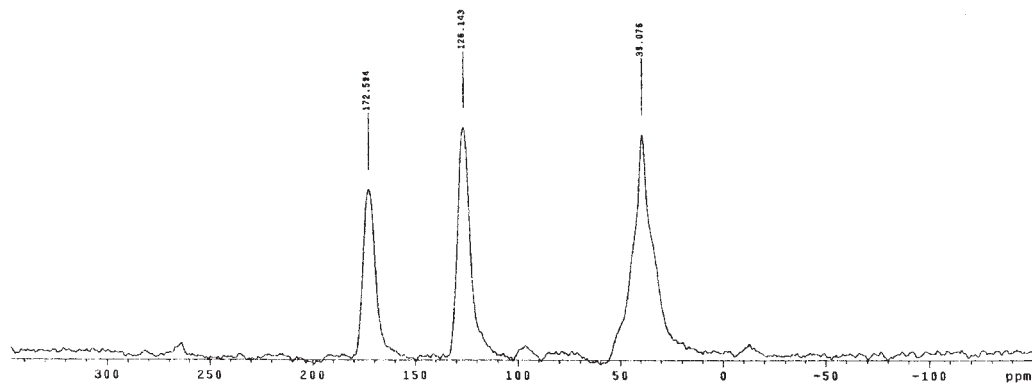


Figure 4 <sup>13</sup>C CPMAS NMR spectrum of pure SMA.

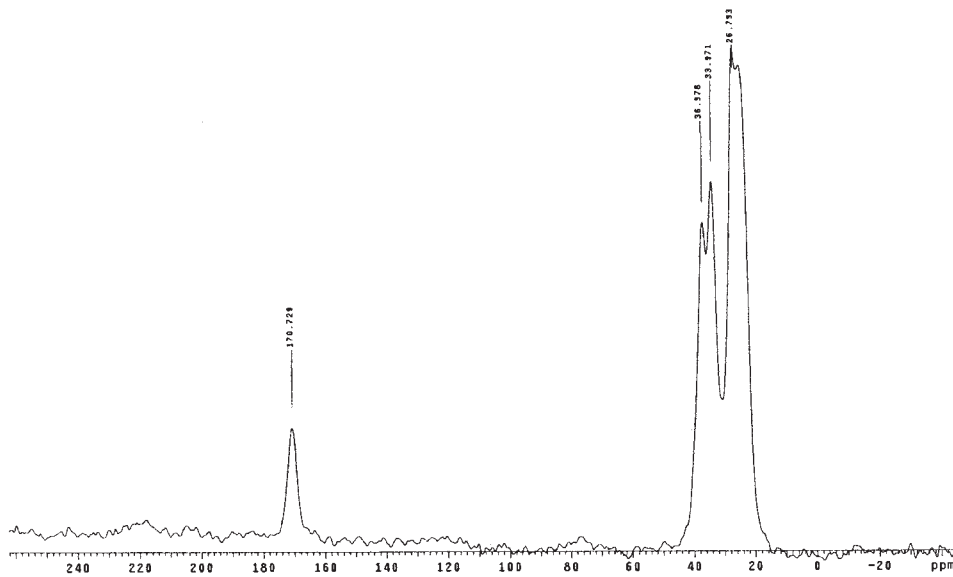


Figure 5 <sup>13</sup>C CPMAS NMR spectrum of pure PA6.

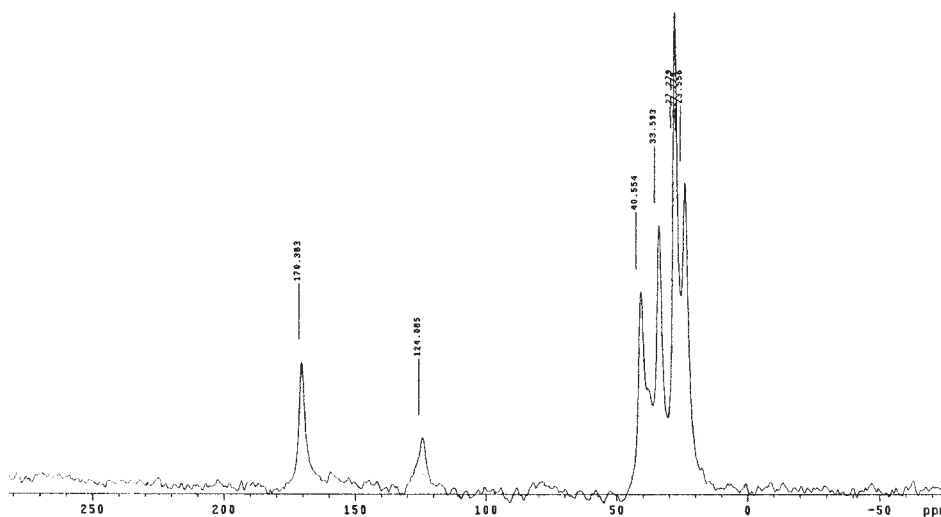


Figure 6  $^{13}\text{C}$  CPMAS NMR spectrum of synthesized SMA-g-PA6 copolymer.

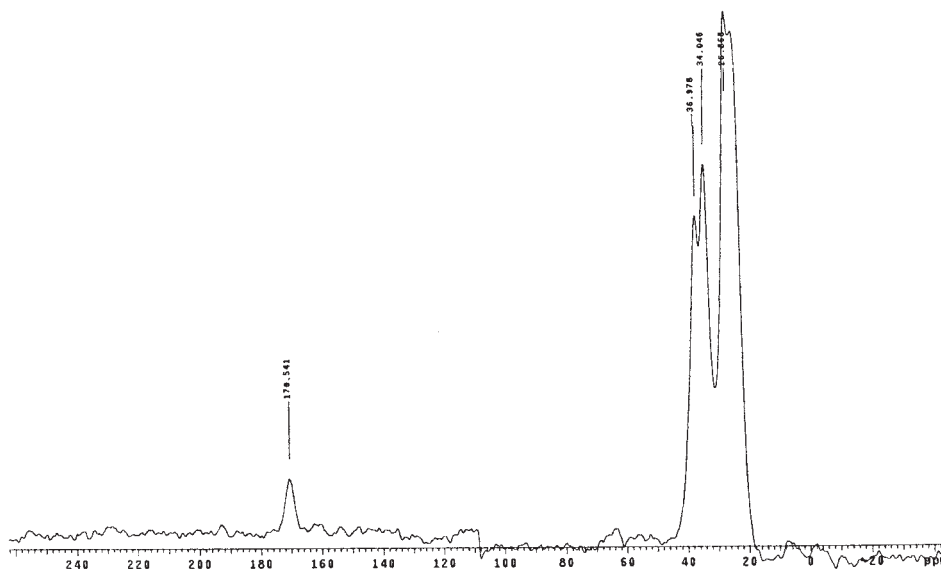


Figure 7  $^{13}\text{C}$  CPMAS NMR spectrum of SMA and PA6 mixer after extraction with a Soxhlet apparatus by acetone.

extracting. Figure 6 suggests that the grafting reaction had taken place between PA6 and SMA.

### DSC analysis

The DSC spectral analysis results are shown in Figure 8. Curves a and b correspond to specimens of SMA-g-PA6 and PA6, respectively. It is observed that the melting point ( $T_m$ ) decreases from 215 to 187°C. The melting point of polymer corresponds to the degree of crystalline order: the higher the crystal defect content, the lower the melting point.<sup>10</sup> This mechanism can be used to explain the melting point decrease of SMA-g-PA6: the grafting reaction affects the mobility of the PA6 chain and destroys the crystalline structure of

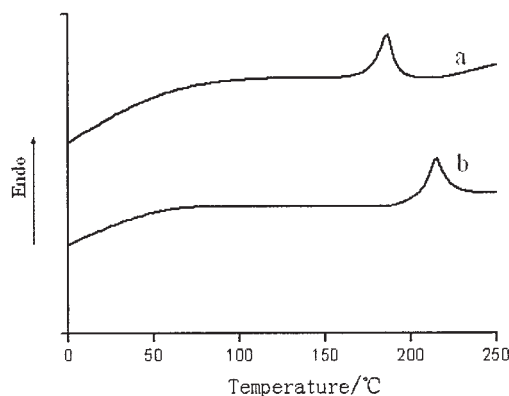
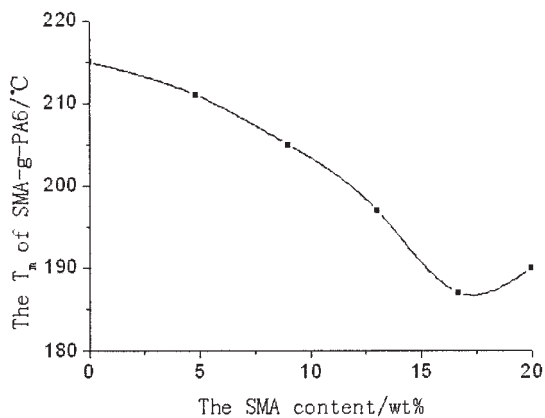


Figure 8 DSC spectra of (a) SMA-g-PA6 copolymer; (b) PA6.



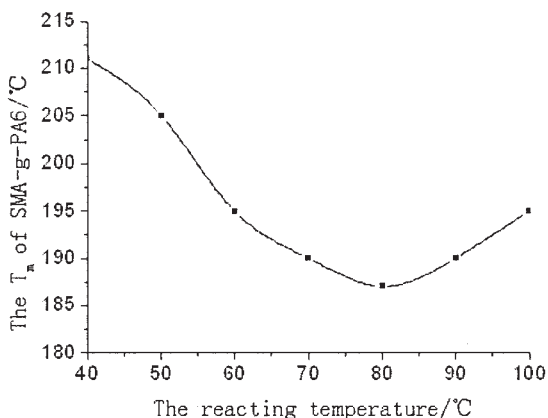
**Figure 9** The  $T_m$  variation of SMA-g-PA6 versus SMA content.

PA6, leading to a lower degree of crystalline order and consequently a lower melting point.

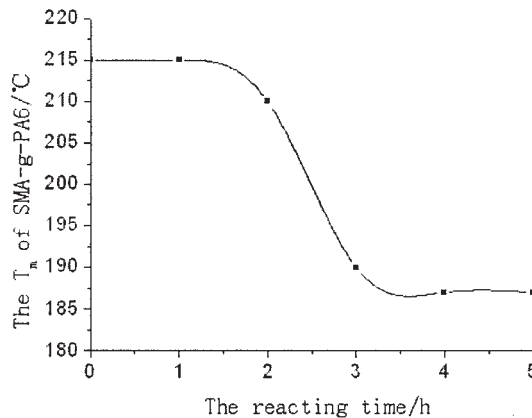
**Melting point analysis of SMA-g-PA6**

Figure 9 shows the variation of the melting point of SMA-g-PA6 as a function of SMA content under the temperature of 80°C for a 4-h residence time. A significant decrease in melting point is observed up to 16 wt % SMA, followed by an increase. The minimum value for the melting point is 187°C. This is an indication of the existence of a critical concentration of SMA, corresponding to 16 wt %.

Figure 10 shows the variation of the melting point of SMA-g-PA6 as a function of reacting temperature, with SMA concentration fixed at 16 wt % and reacting time fixed at 4 h.  $T_m$  decreases with the increase of the reacting temperature up to 80°C, followed by an increase. We think that 80°C appears to be the optimum reacting temperature of SMA to realize minimum  $T_m$ . This is usually attributed to the fact that the meeting frequency of SMA and PA6 increases with increasing



**Figure 10** The  $T_m$  variation of SMA-g-PA6 versus reacting temperature.



**Figure 11** The  $T_m$  variation of SMA-g-PA6 versus reacting time.

temperature, consequently giving a high grafting ratio. Whereas at excess high reacting temperature, the  $\nu$  of the system increases, which reduces meeting frequency of SMA and PA6 molecules, consequently giving a low grafting ratio.

Figure 11 represents the variation of SMA-g-PA6  $T_m$  versus reacting time: SMA concentration was fixed at 16 wt % and the reacting temperature was 80°C. The  $T_m$  decreases slowly up to 2 h reacting time and then sharply up to 3 h reacting time, and then slowly again. This behavior is attributed to the  $\nu$  increase and consequently the reduced grafting ratio during the grafting reaction.

**Performance evaluation of PVC/SMA-g-PA6 blends**

The variation of Izod impact strength with the content of SMA-g-PA6 is illustrated in Figure 12. Curves A, B, and C correspond to PA6 and SMA at the ratios of 5 : 1, 7 : 1, and 10 : 1, respectively. It is noted that impact strength almost doubled for PA6 : SMA = 5 : 1 compared to pure PVC. It increases with the increase of

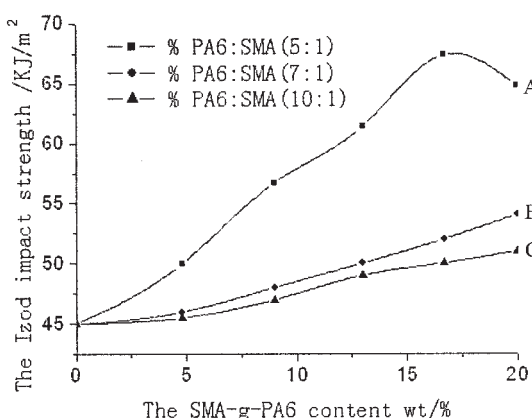


**Figure 12** The Izod impact strength of PVC/SMA-g-PA6 versus SMA-g-PA6 content.

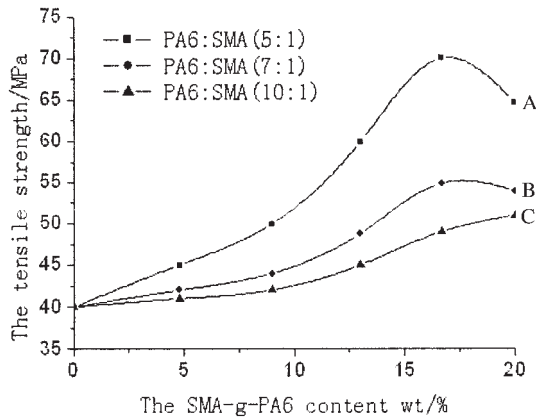


**Figure 13** The tensile strength of PVC/SMA-g-PA6 versus SMA-g-PA6 content.

SMA-g-PA6 concentration, up to 16 wt %, above which it showed a tendency to decrease with the increase of SMA-g-PA6 loading. This is an indication of the presence of a critical SMA-g-PA6 concentration. A significant improvement in impact strength is also observed in curves B and C but less than curve A. This behavior may be attributed to the enhanced interfacial adhesion between PVC and PA6 in the presence of SMA: greater adhesion between the components of the polymer blends yields higher impact strength.

Figure 13 represents the tensile strength of PVC/SMA-g-PA6 versus SMA-g-PA6 content. Curves A, B, and C correspond to the PA6 and SMA at the ratios of 5 : 1, 7 : 1, and 10 : 1. It is interesting to note that in all cases the tensile strength was optimized at 16 wt % SMA-g-PA6 content: the higher the SMA content in SMA-g-PA6, the greater the tensile strength of the blends. The relation between elongation at break and the addition of SMA-g-PA6 is showed in Figure 14. The elongation at break increases with the increase in SMA-g-PA6 content upto 16 wt %. Beyond that, the increase in elongation at break plateaus. It can be

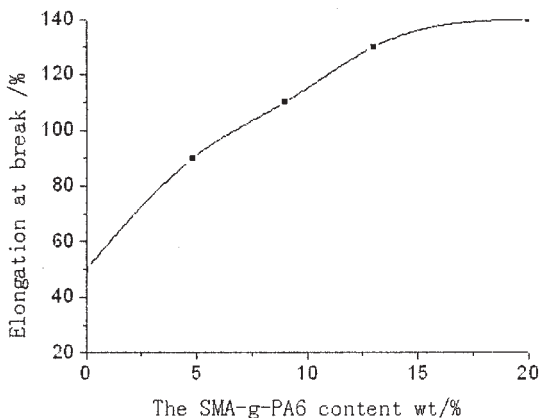
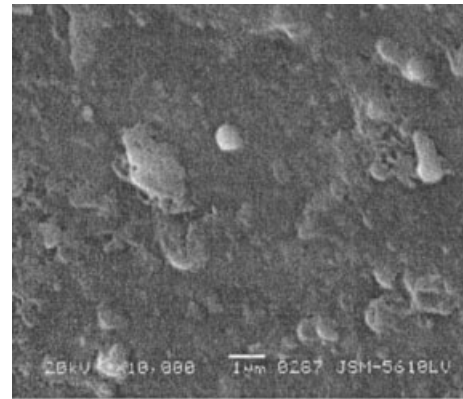
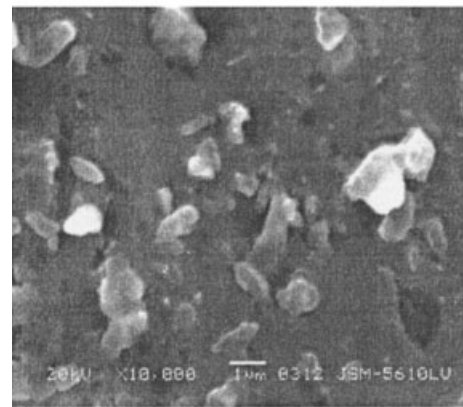


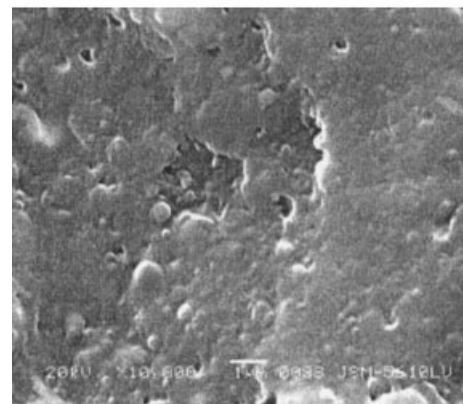
**Figure 14** Elongation at break versus SMA-g-PA6 content.



(a)



(b)



(c)

**Figure 15** The morphology of the PVC/SMA-g-PA6 blends, (a) PVC/PA6/ SMA-g-PA6 = 100: 10 : 0; (b) PVC/SMA-g-PA6 = 100 : 10; (c) PVC/SMA-g-PA6 = 100 : 20.

concluded that 16 wt % SMA-g-PA6 content can be incorporated into PVC to improve the properties such as tensile strength and impact resistance of PVC material for engineering applications.

#### Morphology analysis

The morphology of the blends was investigated by SEM of the impact-fractured surface. For the uncom-

patibilized blends [Fig 15(a)], the size of PA6 domains was not distributed uniformly, and the interfacial adhesion between PA6 and PVC was very weak, as was evident from the easy removal of PA6 particles from the PVC matrix during impact fracture. The compatibilized PVC/SMA-g-PA6 blends, however, show a significant reduction in the domain size compared to the uncompatibilized blends. The average domain size decreased in PVC/SMA-g-PA6 blends with an increase in the level of SMA-g-PA6. The micrographs show two different types of morphology dependent on the SMA-g-PA6 content. A particle-dispersed morphology was observed at SMA-g-PA6 levels lower than 16 wt % [Fig. 15(a,b)], whereas, a cocontinuous morphology was observed at 16 wt % SMA-g-PA6 [Fig. 15 (c)]. The presence of SMA-g-PA6 results in a stable and finer domain size of PA6 and enhanced interfacial adhesion. The cocontinuous morphology leads to high plastic deformability of PVC/SMA-g-PA6 blends. The major mechanism of energy dissipation of PVC/SMA-g-PA6 blends may be multiple crazing due to finely dispersed domain size and shear bands associated with matrix plastic deformation. As a result, the maximum impact strength was 67.3 KJ/m<sup>2</sup> in the PVC/SMA-g-PA6 cocontinuous morphology with a composition ratio of 80 : 20, at which maximum tensile strength was also obtained.

### CONCLUSION

Nylon 6 and PVC are hard to blend because of their poor compatibility and different processing temper-

atures. However, use of a graft copolymer SMA-g-PA6 may resolve this problem as shown in this paper. The graft of SMA onto PA6 in solution can destroy the crystalline structure of PA6, leading to a decrease in crystallinity and consequently a lower melting point. Incorporation of SMA-g-PA6 results in smaller particle size and finer dispersion of PA6 in PVC matrix and gives a cocontinuous morphology to the blends. The change in microstructure is also evidenced by the significant increase in impact and tensile strength.

### ACKNOWLEDGMENT

This work was supported by grant number Z002AA333110 from the National High Technology Research and Development Program of China (863 Program).

### References

1. Hofmann, G. H. U.S. Patent 5352735, 1994.
2. Hofmann, G. H. SPE ANTEC Tech Paper 3380, 1996.
3. Hofmann, G. H. W.O. Patent WO 9708242, 1997.
4. Hofmann, G. H. *Plast Technol* 1998, 6, 55.
5. Hofmann, G. H. George Henry. U.S. Patent 5856405, 1999.
6. Sherman, L. M. *Plast Technol* 1997, 43, 17.
7. Lian, Y. X.; Zhang, Y.; Peng, Z. L.; Zhang, Y. X.; Zhang, X. F.; Yang, J. C. *China Plastic* 2000, 148, 30.
8. Lian, Y. X.; Zhang, Y.; Peng, Z. L.; Zhang, Y. X. *J. SJT University* 2001, 354, 582.
9. Lian, Y. X.; Zhang, Y.; Peng, Z. L.; Zhang, X. F.; Fan, R. L.; Zhang, Y. X. *J Appl Polym Sci* 2001, 80, 2823.
10. Xiong, C. X.; Wang, T.; Liu, Q. H.; Dong, L. J.; Chen, J.; Liu, D. *J Appl Polym Sci* 2004, 91, 563.